ENME 631 – Project Report
Numerical Methods for Engineers
Dec 14, 2021, Virtual, Online
Taught By: Dr. Abdulmajeed Mohamad

THE NUMERICAL SOLUTION OF CHAOS: DOUBLE PENDULUM SYSTEM

Josmar Cristello (UCID: 30158326)
Atul Koshy (UCID: 30149545)
Pipeline Engineering Centre (PEC)
University of Calgary,
Calgary, AB
Canada

ABSTRACT

The simple pendulum has an apparent simple motion, and yet, the union of two pendulums generate a system with a chaotic motion. Although there is no formal proof, there is no known solution for the double pendulum system motion, and thus, it must be solved numerically.

This study aims to analyze such a system and compare the sensitivity to different numerical methods. Moreover, it is also a goal to goal to analyze how the chaotic motion takes place, and whether it is prevalent for the entire system or for some cases.

To achieve that, equations of motion are obtained using the Euler-Lagrangian equation. The resulting differential equations are them solved numerically, using Runge-Kutta (4th order) and Euler's Explicit Forward methods. The system is then computationally simulated using the programming language python. Detailed solutions are initially presented for different initial states of the system and the two different numerical methods, analyzing motion, behavior, and mechanical energy of the system. Then, solutions are presented for a very large number of initial positions, allowing for patterns to be discovered.

Keywords: Numerical Method, Runge-Kutta, Euler, Double Pendulum, Chaotic Motion, Dynamics, Python

NOMENCLATURE

SDP	Simple double pendulum
TFF	Time for First Plot
RK4	Runge-Kutta of fourth order
ODE	Ordinary Differential Equation
$\theta_{1,2}$	Angle of the pendulum with vertical axis
$L_{1,2}$	Length of the connecting rods
$M_{1,2}$	Mass of bobs
$X_{0,1,2}$	X coordinates of the system
$Y_{0,1,2}$	Y coordinates of the system
T	Kinetic energy of the system
V	Potential energy of the system
L	Lagrangian of the system
g	Acceleration due to gravity
h	step height
n	base point
t_n	nth time step

1. INTRODUCTION

Even though a single pendulum is a system with relatively simple motion, the union of two of those pendulums gives rise to a much more interesting system, with a complex, chaotic motion, highly sensitivity to the initial conditions. The planar double pendulum is a system where the first pendulum attached to a pivot on a surface, and the second pendulum is attached to a pivot on the end of the first pendulum. Such a system is illustrated on Figure 1.

This system was first studied by Euler and Daniel Bernoulli in 1738, where governing equations were generalized for n-pendulum systems, and the modes of oscillations were considered [1]. Although there has been no formal proof that those equations can't be solved analytically, many analyses point to that conclusion [2,3]. Because of that, the solutions of those governing equations were only studied in detail hundreds of years later of their initial development, with the invention of computers that were capable of numerically solving them.

Because of its chaotic and nonlinear behavior, the double pendulum system has been widely used to study chaos theory and its resulting systems [4,5]. Besides those applications, it was also used in control theory to develop models to control dynamic systems such as flexible arm robotics [6] and shipboard crane robotics [7]. Finally, this system was also used to study dynamics of biological systems, such as leg swing for human and animal locomotion [8] and the dynamics of an arm swing while playing different sports, such as golf [9], baseball and tennis [10] in order to optimize sport performance.

Throughout this study, the equations of motion for the double pendulum are going to be derived and solved numerically with two different methods: Runge-Kutta (4th order) and Euler Explicit Forward. Moreover, the chaotic motion, and thus, the

sensitivity of the system to the initial conditions are going to be demonstrated.

2. Equations of Motion

To derive the equations of motion, the system is assumed to be undamped with gravity being the only force acting on it. The system consists of two bobs with masses $M_{1,2}$, connected by massless strings, or rods, $L_{1,2}$. The first bob is connected to an immovable pivot at an end, and to the second bob, which is free to rotate. The initial position of the system is then described by their initial angular positions, $\theta_{1,2}$.

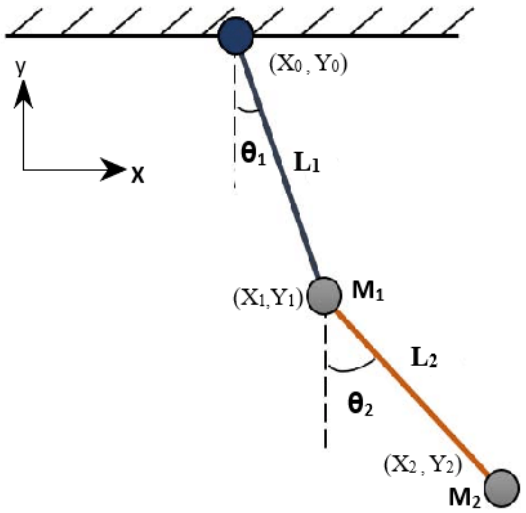

Figure 1. Simple Double Pendulum Forces.

The Trigonometric identities used here are given by:

$\sin^2\theta + \cos^2\theta = 1$
$\sin\theta_1 \cdot \sin\theta_2 + \cos\theta_1 \cdot \cos\theta_2 = \cos(\theta_1 - \theta_2)$

The cartesian coordinates X_1, Y_1, X_2, Y_2 are given by:

$X_1 = L_1\sin\theta_1$ (1)
$Y_1 = -L_1\cos\theta_1$ (2)
$X_2 = L_1\sin\theta_1 + L_2\sin\theta_2$ (3)
$Y_2 = -L_1\cos\theta_1 - L_2\cos\theta_2$ (4)

Their velocities after derivation are given by:

$\dot{X}_1 = \dot{\theta}_1 L_1\cos\theta_1$ (5)
$\dot{Y}_1 = \dot{\theta}_1 L_1\sin\theta_1$ (6)
$\dot{X}_2 = \dot{\theta}_1 L_1\cos\theta_1 + \dot{\theta}_2 L_2\cos\theta_2$ (7)
$\dot{Y}_2 = \dot{\theta}_1 L_1\sin\theta_1 + \dot{\theta}_2 L_2\sin\theta_2$ (8)

The potential energy due to gravity is given below:

$V = M_1 g Y_1 + M_2 g Y_2$ (9)
From equation (2) and (4) we get:
$V = M_1 g[-L_1\cos\theta_1] + M_2 g[-L_1\cos\theta_1 - L_2\cos\theta_2]$
$V = -(M_1 + M_2)gL_1\cos\theta_1 - M_2 g L_2\cos\theta_2$ (10)

The total kinetic energy is given by:

$T = \frac{1}{2}M_1V_1^2 + \frac{1}{2}M_2V_2^2$
$T = \frac{1}{2}M_1(\dot{X}_1^2+\dot{Y}_1^2) + \frac{1}{2}M_2(\dot{X}_2^2+\dot{Y}_2^2)$ (11)

From equation (5) to (8) we get:

$T = \frac{1}{2} M_1[(\dot{\theta}_1 L_1\cos\theta_1)^2 + (\dot{\theta}_1 L_1\sin\theta_1)^2] + \frac{1}{2} M_2[(\dot{\theta}_1 L_1\cos\theta_1 + \dot{\theta}_2 L_2\cos\theta_2)^2 + (\dot{\theta}_1 L_1\sin\theta_1 + \dot{\theta}_2 L_2\sin\theta_2)^2]$
$T = \frac{1}{2} M_1[\dot{\theta}_1^2 L_1^2(\cos^2\theta_1 + \sin^2\theta_1)] + \frac{1}{2} M_2[(\dot{\theta}_1 L_1\cos\theta_1 + \dot{\theta}_2 L_2\cos\theta_2)^2 + (\dot{\theta}_1 L_1\sin\theta_1 + \dot{\theta}_2 L_2\sin\theta_2)^2]$
$T = \frac{1}{2} M_1[\dot{\theta}_1^2 L_1^2] + \frac{1}{2} M_2[\dot{\theta}_1^2 L_1^2\cos^2\theta_1 + \dot{\theta}_2^2 L_2^2\cos^2\theta_2 + 2\dot{\theta}_1 L_1\cos\theta_1\dot{\theta}_2 L_2\cos\theta_2 + \dot{\theta}_1^2 L_1^2\sin^2\theta_1 + \dot{\theta}_2^2 L_2^2\sin^2\theta_2 + 2\dot{\theta}_1 L_1\sin\theta_1\dot{\theta}_2 L_2\sin\theta_2]$
$T = \frac{1}{2} M_1[\dot{\theta}_1^2 L_1^2] + \frac{1}{2} M_2[(\dot{\theta}_1^2 L_1^2(\sin^2\theta_1 + \cos^2\theta_1)) + (\dot{\theta}_2^2 L_2^2(\sin^2\theta_2 + \cos^2\theta_2)) + 2L_1L_2\dot{\theta}_1\dot{\theta}_2(\cos\theta_1\cos\theta_2 + \sin\theta_1\sin\theta_2)]$
$T = \frac{1}{2} M_1[\dot{\theta}_1^2 L_1^2] + \frac{1}{2} M_2[\dot{\theta}_1^2 L_1^2 + \dot{\theta}_2^2 L_2^2 + 2L_1L_2\dot{\theta}_1\dot{\theta}_2(\cos\theta_1\cos\theta_2 + \sin\theta_1\sin\theta_2)]$
$T = \frac{1}{2} M_1[\dot{\theta}_1^2 L_1^2] + \frac{1}{2} M_2[\dot{\theta}_1^2 L_1^2 + \dot{\theta}_2^2 L_2^2 + 2L_1L_2\dot{\theta}_1\dot{\theta}_2\cos(\theta_1 - \theta_2)]$ (12)

The Lagrangian for the system can be found by using the equation of the motion of the system in terms of generalized coordinates:

$L = T - V$ (13)

where T represents the kinetic energy and V represents potential energy.

Substituting equation (12) and (10) in (13):

$L = \frac{1}{2} M_1[\dot{\theta}_1^2 L_1^2] + \frac{1}{2} M_2[\dot{\theta}_1^2 L_1^2 + \dot{\theta}_2^2 L_2^2 + 2L_1L_2\dot{\theta}_1\dot{\theta}_2\cos(\theta_1 - \theta_2)] + (M_1 + M_2)gL_1\cos\theta_1 + M_2 g L_2\cos\theta_2$ (14)

Lagrange's equation:

$\frac{\partial}{\partial t}\left(\frac{\partial L}{\partial \dot{q}_i}\right) - \left(\frac{\partial L}{\partial q_i}\right) = 0$ (15)

Solving in the first direction of motion:

θ_1 :

$$\frac{\partial L}{\partial \dot{\theta 1}} = \frac{\partial}{\partial \theta 1}[½M_1L_1^2\dot{\theta}_1^2 + ½M_2L_1^2\dot{\theta}_1^2 + ½M_22L_1L_2\dot{\theta}_1\dot{\theta}_2\cos(\theta_1 - \theta_2)]$$

$$\frac{\partial L}{\partial \dot{\theta 1}} = M_1L_1^2\dot{\theta}_1 + M_2L_1^2\dot{\theta}_1 + M_2L_1L_2\dot{\theta}_2\cos(\theta_1 - \theta_2) \quad (16)$$

$$\frac{\partial}{\partial t}\left(\frac{\partial L}{\partial \dot{\theta 1}}\right) = (M_1 + M_2)L_1^2\ddot{\theta}_1 + M_2L_1L_2\ddot{\theta}_2\cos(\theta_1 - \theta_2) - M_2L_1L_2\dot{\theta}_2\sin(\theta_1 - \theta_2)(\dot{\theta}_1 - \dot{\theta}_2) \quad (17)$$

$$\frac{\partial L}{\partial \theta 1} = \frac{\partial}{\partial \theta 1}[½M_22L_1L_2\dot{\theta}_1\dot{\theta}_2\cos(\theta_1 - \theta_2) + (M_1 + M_2)gL_1\cos\theta_1]$$

$$\frac{\partial L}{\partial \theta 1} = -M_2L_1L_2\dot{\theta}_1\dot{\theta}_2\sin(\theta_1 - \theta_2) - (M_1 + M_2)gL_1\sin\theta_1 \quad (18)$$

Putting the equation (17) and (18) in (15)

$$(M_1 + M_2)L_1^2\ddot{\theta}_1 + M_2L_1L_2\ddot{\theta}_2\cos(\theta_1 - \theta_2) - M_2L_1L_2\dot{\theta}_2\sin(\theta_1 - \theta_2)(\dot{\theta}_1 - \dot{\theta}_2) + M_2L_1L_2\dot{\theta}_2\dot{\theta}_1\sin(\theta_1 - \theta_2) + (M_1 + M_2)gL_1\sin\theta_1 = 0$$

$$(M_1 + M_2)L_1^2\ddot{\theta}_1 + M_2L_1L_2\ddot{\theta}_2\cos(\theta_1 - \theta_2) - M_2L_1L_2\dot{\theta}_1\dot{\theta}_2\sin(\theta_1 - \theta_2) + M_2L_1L_2\dot{\theta}_2^2\sin(\theta_1 - \theta_2) + M_2L_1L_2\dot{\theta}_2\dot{\theta}_1\sin(\theta_1 - \theta_2) + (M_1 + M_2)gL_1\sin\theta_1 = 0$$

$$(M_1 + M_2)L_1^2\ddot{\theta}_1 + M_2L_1L_2\ddot{\theta}_2\cos(\theta_1 - \theta_2) + M_2L_1L_2\dot{\theta}_2^2\sin(\theta_1 - \theta_2) + (M_1 + M_2)gL_1\sin\theta_1 = 0$$

$$(M_1 + M_2)L_1\ddot{\theta}_1 + M_2L_2\ddot{\theta}_2\cos(\theta_1 - \theta_2) + M_2L_2\dot{\theta}_2^2\sin(\theta_1 - \theta_2) + (M_1 + M_2)g\sin\theta_1 = 0 \quad (19)$$

θ_2 :

$$\frac{\partial L}{\partial \dot{\theta 2}} = \frac{\partial}{\partial \theta 2}[½M_2L_2^2\dot{\theta}_2^2 + 2L_1L_2\dot{\theta}_1\dot{\theta}_2\cos(\theta_1 - \theta_2)]$$

$$\frac{\partial L}{\partial \dot{\theta 2}} = M_2L_2^2\dot{\theta}_2 + ½M_2L_1L_2\dot{\theta}_1\cos(\theta_1 - \theta_2)$$

$$\frac{\partial L}{\partial \dot{\theta 2}} = M_2L_2^2\dot{\theta}_2 + M_2L_1L_2\dot{\theta}_1\cos(\theta_1 - \theta_2) \quad (20)$$

$$\frac{\partial}{\partial t}\left(\frac{\partial L}{\partial \dot{\theta 2}}\right) = M_2L_2^2\ddot{\theta}_2 + M_2L_1L_2\ddot{\theta}_1\cos(\theta_1 - \theta_2) - M_2L_1L_2\dot{\theta}_1\sin(\theta_1 - \theta_2)(\dot{\theta}_1 - \dot{\theta}_2) \quad (21)$$

$$\frac{\partial L}{\partial \theta 2} = \frac{\partial}{\partial \theta 2}[½M_22L_1L_2\dot{\theta}_1\dot{\theta}_2\cos(\theta_1 - \theta_2) + M_2gL_2\cos\theta_2]$$

$$\frac{\partial L}{\partial \theta 2} = M_2L_1L_2\dot{\theta}_1\dot{\theta}_2\sin(\theta_1 - \theta_2) - M_2gL_2\sin\theta_2 \quad (22)$$

Putting the equation (21) and (22) in equation (15)

$$M_2L_2^2\ddot{\theta}_2 + M_2L_1L_2\ddot{\theta}_1\cos(\theta_1 - \theta_2) - M_2L_1L_2\dot{\theta}_1\sin(\theta_1 - \theta_2)(\dot{\theta}_1 - \dot{\theta}_2) - M_2L_1L_2\dot{\theta}_1\dot{\theta}_2\sin(\theta_1 - \theta_2) + M_2gL_2\sin\theta_2 = 0$$

$$M_2L_2^2\ddot{\theta}_2 + M_2L_1L_2\ddot{\theta}_1\cos(\theta_1 - \theta_2) - M_2L_1L_2\dot{\theta}_1^2\sin(\theta_1 - \theta_2) + M_2L_1L_2\dot{\theta}_1\dot{\theta}_2\sin(\theta_1 - \theta_2) - M_2L_1L_2\dot{\theta}_1\dot{\theta}_2\sin(\theta_1 - \theta_2) + M_2gL_2\sin\theta_2 = 0$$

$$M_2L_2^2\ddot{\theta}_2 + M_2L_1L_2\ddot{\theta}_1\cos(\theta_1 - \theta_2) - M_2L_1L_2\dot{\theta}_1^2\sin(\theta_1 - \theta_2) + M_2gL_2\sin\theta_2 = 0 \quad (23)$$

3. Methodology – Numerical Methods

As mentioned before, there is no known analytical solution for the double pendulum motion. Because of that, it must be solved numerically. Lagrangian equation, for example, offers both verification and comparison of methods such as Euler, Hamilton and Runge-Kutta [11].

3.1 Runge – Kutta 4th Order

Runge-Kutta method was developed by the German mathematicians' Carl Runge and Wilhelm Kutta in 1900s. The Runge-Kutta method finds approximate value of y for a given value of x. Only first order ordinary differential equations can be solved using the RK4 method [12]. The basic idea of Runge-Kutta method is to eliminate the error terms order by order. The fourth order Runge-Kutta method can be expressed as follows:

$$y_{n+1} = y_n + \frac{1}{6}(\Delta y_1 + 2\Delta y_2 + 2\Delta y_3 + \Delta y_4) \quad (24)$$

By defining the step height (h) and $t_n = t_0 + nh$. The following formula can be expressed as:

$$\Delta y_1 = hf(t_n, y_n) \quad (25a)$$

$$\Delta y_2 = hf(t_n + \frac{h}{2}, y_n + \frac{\Delta y1}{2}) \quad (25b)$$

$$\Delta y_3 = hf(t_n + \frac{h}{2}, y_n + \frac{\Delta y2}{2}) \quad (25c)$$

$$\Delta y_4 = hf(t_n + h, y_n + \Delta y_3) \quad (25d)$$

In order to perform the consistency and order analysis and stability analysis on RK4 method, the above equations must be applied to a model ODE, $\bar{y}' + \alpha\bar{y} = 0$, for which $f(t, \bar{y}) = -\alpha\bar{y}$, and the result must be combined into a single-step FDE. Thus,

$$\Delta y_1 = hf(t_n, y_n) = h(-\alpha y_n) = -(\alpha h)y_n \quad (26)$$

$$\Delta y_2 = hf(t_n + \frac{h}{2}, y_n + \frac{\Delta y1}{2}) = h(-\alpha\{y_n + ½[-(\alpha h)y_n]\}) \quad (27a)$$

$$\Delta y_2 = -(\alpha h)y_n(1 - \frac{(\alpha h)}{2}) \quad (27b)$$

$$\Delta y_3 = hf(t_n + \frac{h}{2}, y_n + \frac{\Delta y2}{2}) = h(-\alpha\{y_n + \frac{1}{2}[-(\alpha h)y_n(1 - \frac{(\alpha h)}{2})]\}) \quad (28a)$$

$$\Delta y_3 = -(\alpha h)y_n[1 - \frac{(\alpha h)}{2} + \frac{(\alpha h)^2}{4}] \quad (28b)$$

$$\Delta y_4 = hf(t_n + h, y_n + \Delta y_3) = h(-\alpha\{y_n + [-(\alpha h)y_n(1 - \frac{(\alpha h)}{2} + \frac{(\alpha h)^2}{4})]\}) \quad (29a)$$

$$\Delta y_4 = -(\alpha h)y_n[1 - (\alpha h) + \frac{(\alpha h)^2}{2} + \frac{(\alpha h)^3}{4}] \quad (29b)$$

Substituting Eqs. (26). (27b), (28b) and (29b) into Eq. (24) gives the single step FDE corresponding to Eqs. (24) and (25)

$$y_{n+1} = y_n - (\alpha h)y_n + \frac{1}{2}(\alpha h)^2y_n - \frac{1}{6}(\alpha h)^3y_n + \frac{1}{24}(\alpha h)^4y_n \quad (30)$$

3.2 Euler Method

In the mid-1750s, Swiss mathematician Leonhard Euler devised the Euler method. Euler's technique is a first-order numerical procedure for solving ODEs with a given starting boundary condition [13]. The method's local error (error in each step) is proportional to the step size squared, whereas the global error (error over time) is proportional to the step height. Euler's approach is frequently used as a foundation for more advanced procedures.

Let us denote the time at the nth time-step by t_n and the computed solution at the nth time-step by y_n i.e. $y_n \equiv y(t = t_n)$. The step height h, which is assumed to be constant for simplicity, is then given by $h = t_n - t_{n-1}$. Given (t_n, y_n), the forward Euler method computes y_{n+1} as

$$y_{n+1} = y_n + hf(y_n, t_n) \text{ (Explicit Forward Euler Method)} \quad (31)$$

The forward Euler method is based on a truncated Taylor series expansion, i.e., if we expand y in the neighborhood of $t = t_n$, we get:

$$y(t_n + h) = y_{n+1} = y(t_n) + h\frac{dy}{dt}|_{tn} + O(h^2) = y_n + hf(y_n, t_n) + O(h^2) \quad (32)$$

3.3 Algorithm Development

Algorithms were developed to implement both Runge-Kutta 4th order and Explicit Forward Euler Methods using the programming language Python v3.9.7. The algorithms were also tested with equations that have analytical solutions. The tests and the detailed description of the python code and files can be found on the annex. Additionally, the code has been made open source under the MIT license for educational use and can be found on https://github.com/notidentical/Double-Pendulum-Simulation.

4. Numerical Solution

After solving equations (23) for the angular positions of both bobs ($\theta_{1,2}$) and angular velocities ($\omega_{1,2}$), a few extra derived parameters are calculated as well. Those are going to be derived here. First, the cartesian horizontal ($x_{1,2}$) and vertical coordinates ($y_{1,2}$) are calculated for all time intervals, as per equations 1 through 4. Then, the kinetic ($K_{1,2}$), potential ($U_{1,2}$) and total mechanical energy (M_{Eng}) is also calculated for both bobs using equations 9 through 11.

The simulations were integrated for an initial time of 0 seconds (t_i), final time of 10 seconds (t_f), with an incrementing interval of 0.025 seconds (Δ_t).

4.1 System Sensitivity to Initial Conditions

To determine the sensitivity of the double pendulum system to the initial conditions, two cases were selected. The first case consists of a mass of 1 kg for the first bob (m_1) and 0.5 kg for the second bob (m_2). The length of the wire to the first bob is 1 m (L_1) and to the second bob is 1.5 m (L_2). The first bob starts with an angle of 0.8π radians (θ_1), and the second bob with an angle of -1.2π radians (θ_2). Finally, both bobs start with a null angular velocity ($\dot{\theta}_{1,2}$). The second case has the first bob starting with an angular position 0.8% larger (θ_2), but all other conditions are the same. Those conditions are going to be referenced throughout this study, and thus, are displayed in Table 1 for reference.

Table 1. Initial Values for Case 1 and 2.

Variable	Case 1	Case 2
Bob #1 – Mass (M_1)	1.0 kg	
Bob #2 – Mass (M_2)	0.5 kg	
Bob #1 – Length (L_1)	1.0 m	
Bob #2 – Length (L_2)	1.5 m	
Bob #1 – A. Velocity ($\dot{\theta}_1$)	0 rad/s	
Bob #2 – A. Velocity ($\dot{\theta}_2$)	0 rad/s	
Bob #1 – Angle (θ_1)	0.8π rad	0.8064π rad
Bob #2 – Angle (θ_2)	-1.2π rad	

The cartesian motion (horizontal and vertical) throughout the 10 seconds of simulation is displayed in Figure 2 for cases 1 and 2.

It is particularly interesting how the motion starts almost the same, but quickly diverges to dramatically different paths. In other words, a very small difference in the starting angular position (0.08%) is enough to generate a completely different motion. This is one of the most prominent hallmarks of chaotic behavior [14].

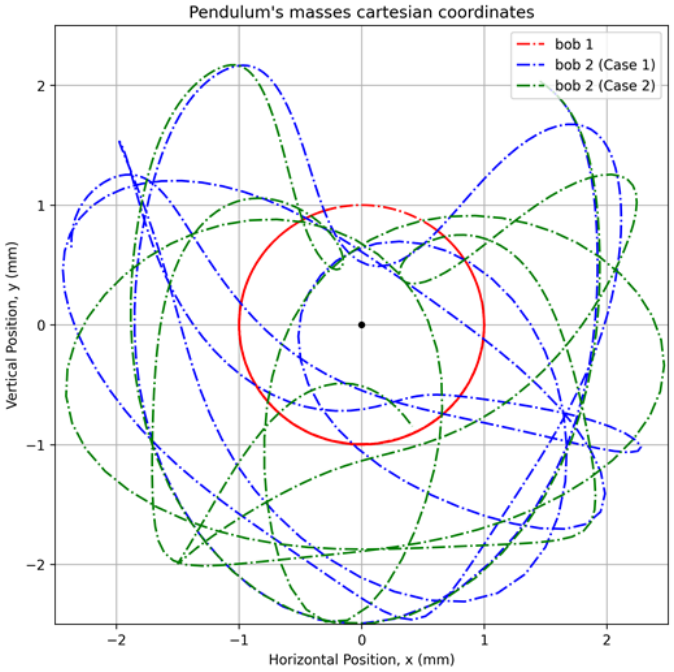

Figure 2. Comparison of motion – Case 1 and 2. Solved with Runge-Kutta 4th order.

Besides the different trajectories, it should also be noticed that the number of flips is completely different for the two cases.

For the first case, bob #2 flips a total of 4 times, whereas for the second case, bob #2 flips only two times. The number of flips is going to be explored in much more detail later.

4.2 System Sensitivity to Numerical Algorithm

To the sensitivity of the system to the numerical method algorithm, in this section case 1 was solved with both Runge-Kutta 4th order (RK4) and the Explicit Forward Euler Method. The results are displayed on Figure 3.

Similar to when the initial conditions were changed, the resulting motions were once again different. For this case, the difference in trajectories was even more extreme, for RK4 the bob #2 flips 4 times (it is the same simulation as before), whereas for Euler method it flips a total of 9 times.

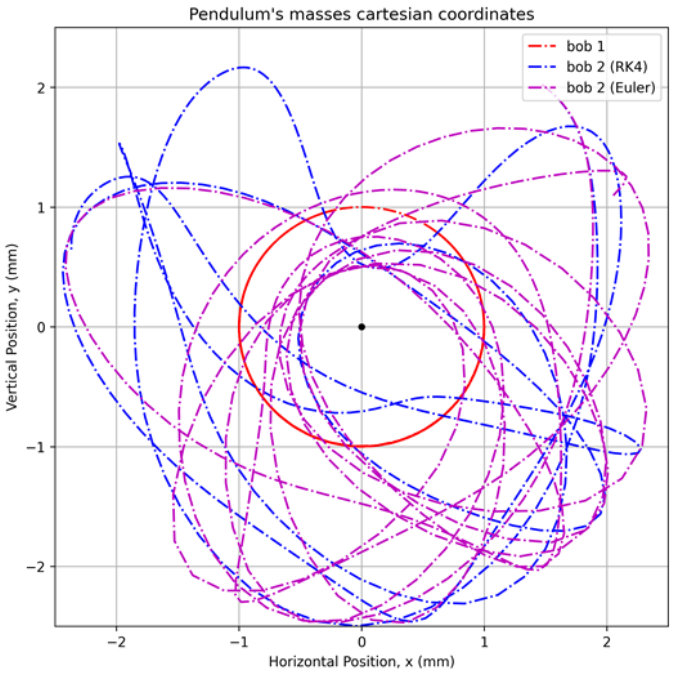

Figure 3. Comparison of motion – RK4 and Euler.

4.3 Mechanical Energy of the System

Since there is no known analytical solution to the double pendulum system, one way to verify the numerical methods selected is to analyze its mechanical energy. Since the system is being simulated as non-damped, frictionless system without air resistance or any other dissipative forces, it is expected the mechanical energy to be conserved (i.e., constant) throughout the entire motion time.

The mechanical energy for bob#1, bob#2 and for the whole system with RK4 method are computed and shown on Figure 4. It is possible to see how the energy of the system is almost constant, and that the bobs behave symmetrically - that is, when the energy of bob 1 drops, the energy of bob 2 increases, and vise-versa. The symmetry also gives merit to the physical derivation, as the conservation of energy implies that any drops and gains in energy are conversions between potential and kinetic energy between the two bobs.

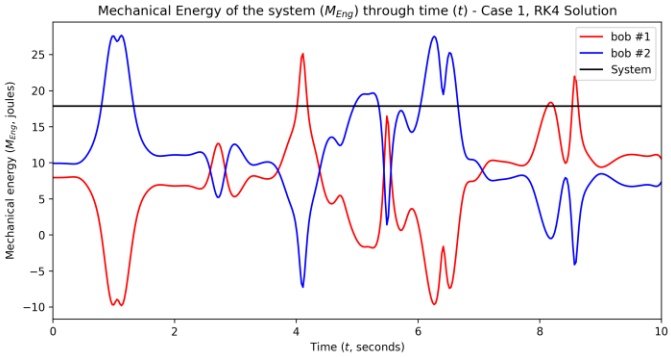

Figure 4. Mechanical Energy – Case 1, RK4.

Then, the mechanical energy for the two bobs and the system with Euler's method is shown in Figure 5. For this case, the bobs still behave in an apparently symmetrical way, but ultimately the mechanical energy increases significantly. This is not surprising, as any numerical method is introducing some degree of error.

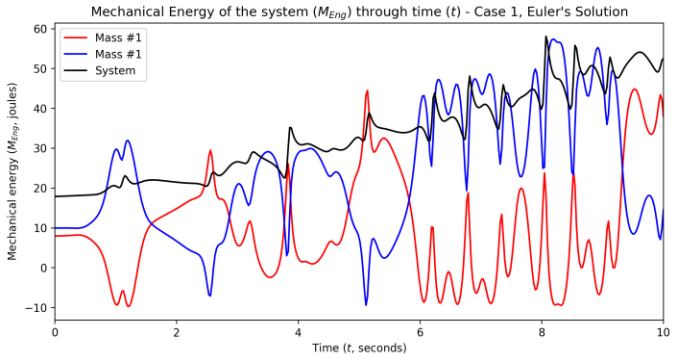

Figure 5. Mechanical Energy – Case 1, Euler.

It is hard to see in Figure 4 the energy variation for the RK4 solution, since it is just a small fraction of the initial value. To be precise, the variation for RK4 was of -0.008J, a 0.04% decrease from the initial energy. In comparison, Euler method had a variation of 34J, a 194% increase from the initial value. This difference is displayed in Figure 6.

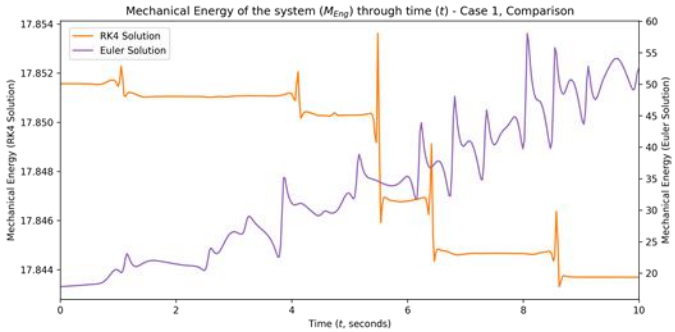

Figure 6. Total Mechanical Energy – Comparison.

5. Chaotic Behavior

The previous section briefly analyzed two cases and demonstrated the sensitivity to initial conditions. This section will analyze this phenomenon for a much larger number of initial values, to see whether this is present for the entire angular spectrum of angular positions. Since it was found that the mechanical energy conservation for Euler's method was not respect, and thus, is not accepted, the rest of the study will be carried out exclusively with RK4.

5.1 Number of Flips - Second Bob

A flip can be defined in different ways, but for the purposes of this analysis it will be defined as a bob radially dislocating a full revolution (i.e., 2.0π rad) in either direction. Furthermore, the absolute rotation is going to be considered, so if a bob flips once in the clockwise direction and once in the counterclockwise direction, it will be computed as two flips. Finally, the angular revolution is not referential, so each bob flip is computed individually.

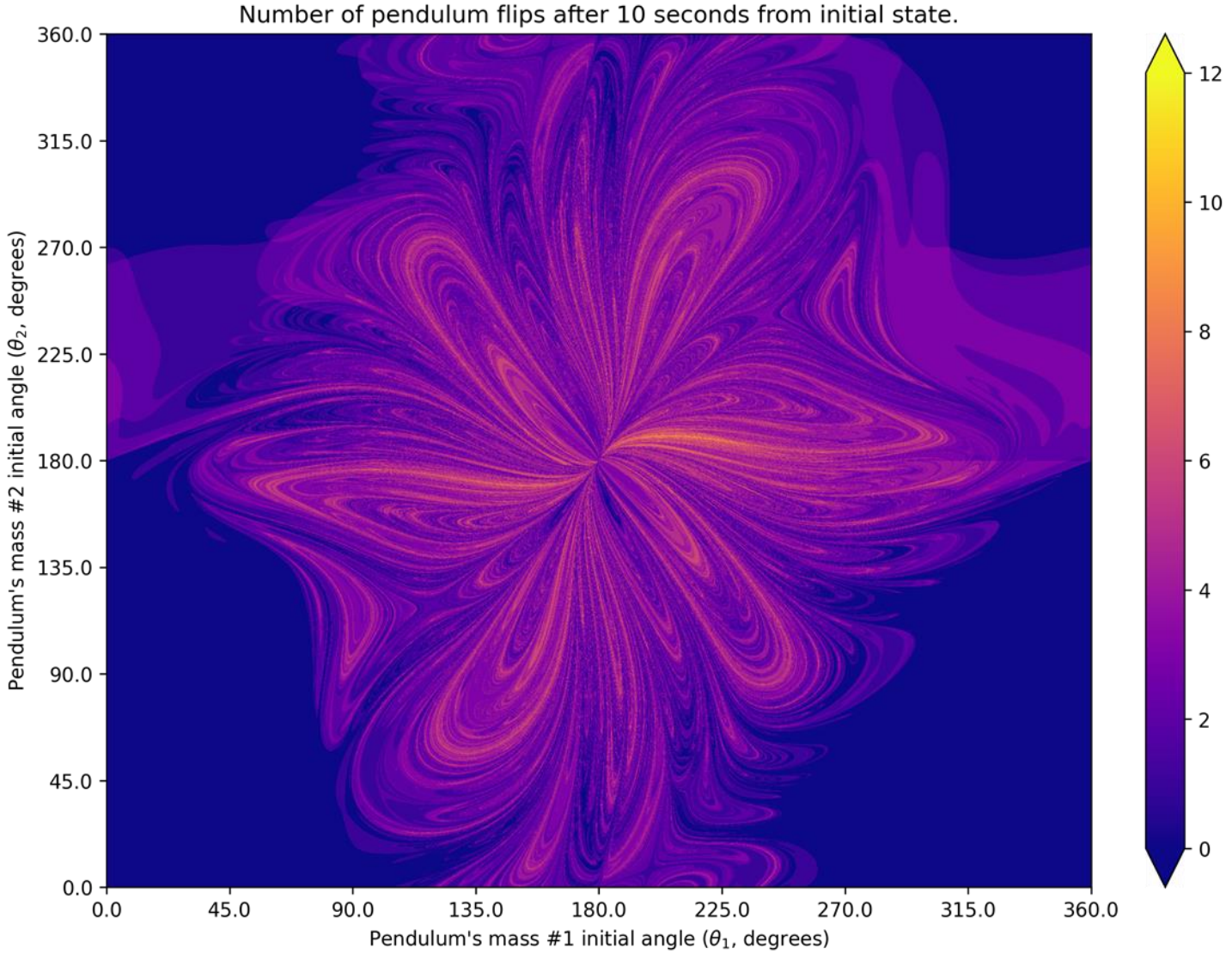

Figure 7. Number of pendulum's bob# 2 flips after 10 seconds of motion, for different bob 1 and 2 initial angles.

For Figure 7, the initial angular position of bobs #1 and #2 are iterated from 0 to 2π radians in 1500 steps each, for a total of 1500^2 = 2,250,000 individual trajectories simulated. For each pair of position, the color represents the number of bob #2 flips during the 10 seconds of motion.

This allows for many this interesting, chaotic behavior to be seen in more detail. For the four edges of the image, places where the initial angular position of either bob is closer to either 0 or 2π radians, the bob does not flip at all. This is not surprising, as other studies found that for small angles the system tends to behave much like a linear oscillator, with almost constant amplitude and period [15].

Closer to the center however, the number of flips varies drastically, with a trajectory with 12 flips almost neighboring another with 0 flips. Interesting patterns can also be seen with strong rotational symmetries, and fractal like properties.

5.2 Final Angular Position - Second Bob

Another way to analyze the chaotic behavior of the system is to look at the final position of either bob 1 or 2. Which, this section chose to study the final position of bob 2 ($\theta_{2,final}$). Much like the previous section, the same 2,250,000 individual trajectories are computed after 10 seconds or simulation for varying initial angular positions of the two bobs. The results are shown on Figure 8.

Once again, the chaotic behavior of the system is prominently displayed. The four corners have a homogenous color gradient, which indicate that the final angular position of bob 2 changes in an almost linear, homogenous way. For the middle of the chart, however, the position changes quickly and drastically, and shares many of the rotation symmetries of Figure 7 , where the number of flips changed from 0 to 12 for relatively close initial conditions.

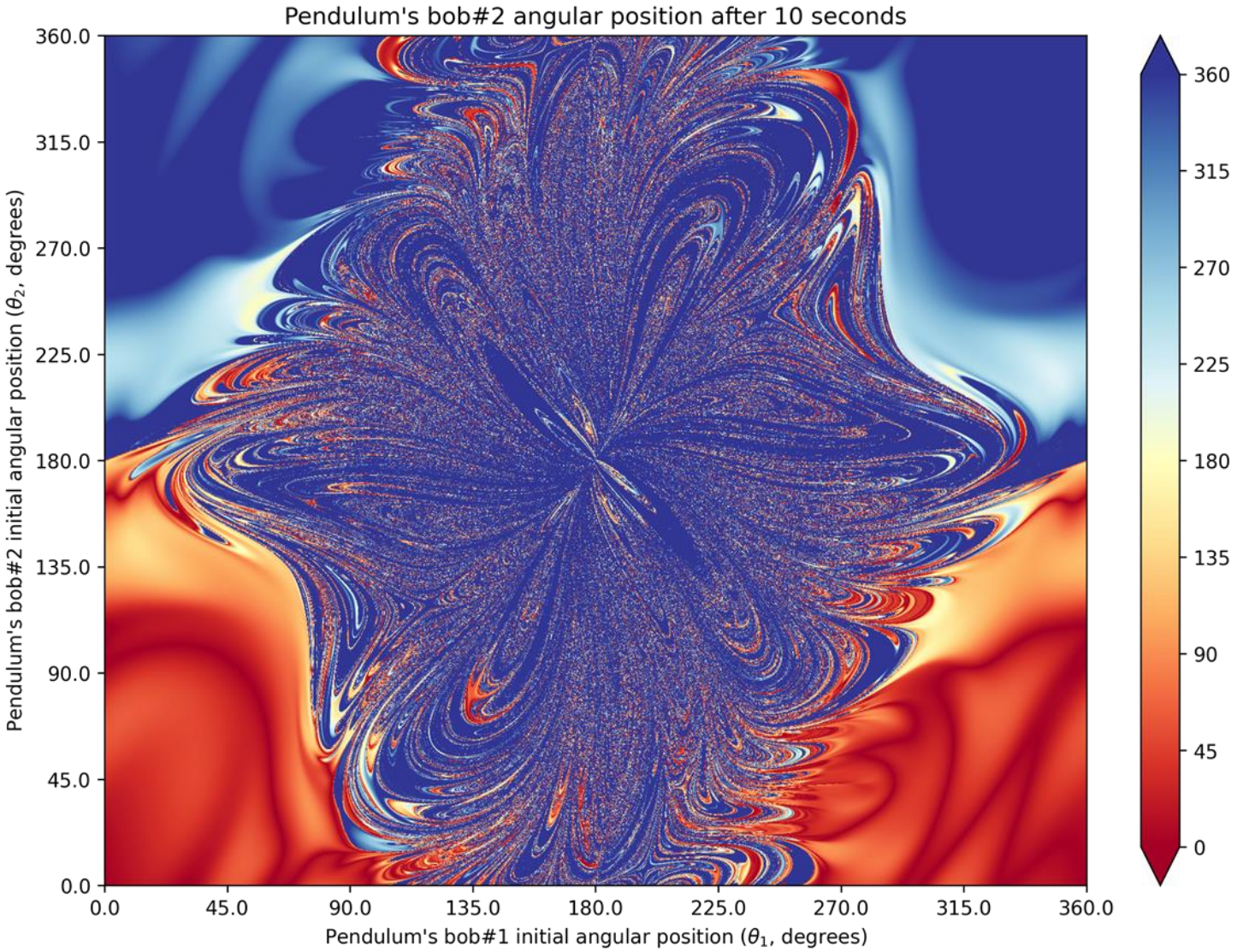

Figure 8. Pendulum's bob 2 position after 10 seconds.

6. Conclusions

This study explored the solution of the double pendulum system – a system that has no known analytical solution - with two different numerical methods: Runge-Kutta 4th order and Euler Explicit Forward. The equations were derived with the Euler-Lagrangian equation. It was shown that the mechanical energy of Runge-Kutta 4th order was conserved to a higher degree than Euler's method.

The chaotic nature of the double pendulum was explored and demonstrated for different parameters. It was shown in detail how, for similar initial positions, the system produces drastically different number of flips and final bob positions. It was also shown that, even though the system is chaotic, it has regions where it behaves in an orderly way.

REFERENCES

1. Acheson, D. J. (1997). *From calculus to chaos: An introduction to dynamics*. Oxford University Press.
2. Stachowiak, T., & Okada, T. (2006). A numerical analysis of chaos in the double pendulum. *Chaos, Solitons & Fractals*, *29*(2), 417–422. https://doi.org/10.1016/j.chaos.2005.08.032
3. Ohlhoff, A., & Richter, P. H. (2000). Forces in the Double Pendulum. *ZAMM*, *80*(8), 517–534. https://doi.org/10.1002/1521-4001(200008)80:8<517::AID-ZAMM517>3.0.CO;2-1
4. Marcelo Tusset, A., Piccirillo, V., Bueno, A. M., Manoel Balthazar, J., Sado, D., Felix, J. L. P., & Brasil, R. M. L. R. da F. (2016). Chaos control and sensitivity analysis of a double pendulum arm excited by an RLC circuit based nonlinear shaker. *Journal of Vibration and Control*, *22*(17), 3621–3637. https://doi.org/10.1177/1077546314564782
5. Sanjeewa, S. D., & Parnichkun, M. (2019). Control of rotary double inverted pendulum system using mixed sensitivity H∞ controller. *International Journal of Advanced Robotic Systems*, *16*(2), 172988141983327. https://doi.org/10.1177/1729881419833273
6. Kiyoumarsi, A., Ataei, M., Mirzaeian-Dehkordi, B., & Ashrafi, R. (2007). The Mathematical Modeling of a Double-Pendulum System as a Physical Model of Flexible Arm Robot. *2007 IEEE International Conference on Control and Automation*, 1900–1904. https://doi.org/10.1109/ICCA.2007.4376692
7. Sun, N., Wu, Y., Liang, X., & Fang, Y. (2019). Nonlinear Stable Transportation Control for Double-Pendulum Shipboard Cranes With Ship-Motion-Induced Disturbances. *IEEE Transactions on Industrial Electronics*, *66*(12), 9467–9479. https://doi.org/10.1109/TIE.2019.2893855
8. Bazargan-Lari, Y., Eghtesad, M., Khoogar, A., & Mohammad-Zadeh, A. (2014). Dynamics and regulation of locomotion of a human swing leg as a double-pendulum considering self-impact joint constraint. *Journal of Biomedical Physics & Engineering*, *4*(3), 91–102.
9. Inoue, Y., Shibata, K., Fukumoto, M., Wang, S., & Oka, K. (n.d.). *Study on Dynamic Analysis and Wearable Sensor System for Golf Swing*. 146.
10. Neal, H. (n.d.). *Using Mechanics of a Double Pendulum to Maximize Sport Performance*. 6.
11. Gonzalez, G. (2008). *Single and Double plane pendulum*. 8.
12. Zingg, D. W., & Chisholm, T. T. (1999). Runge–Kutta methods for linear ordinary differential equations. *Applied Numerical Mathematics*, *31*(2), 227–238. https://doi.org/10.1016/S0168-9274(98)00129-9
13. J, R. (1983). *Runge-kutta method. Numerical Methods.*
14. Levien, R. B., & Tan, S. M. (1998). Double pendulum: An experiment in chaos. *American Journal of Physics*, *61*(11), 1038. https://doi.org/10.1119/1.17335
15. Chen, Joe. (2008). *Chaos from Simplicity: An Introduction to the Double Pendulum*.

APPENDIX

APPENDIX 1. Demonstration of Numerical Method Implementation

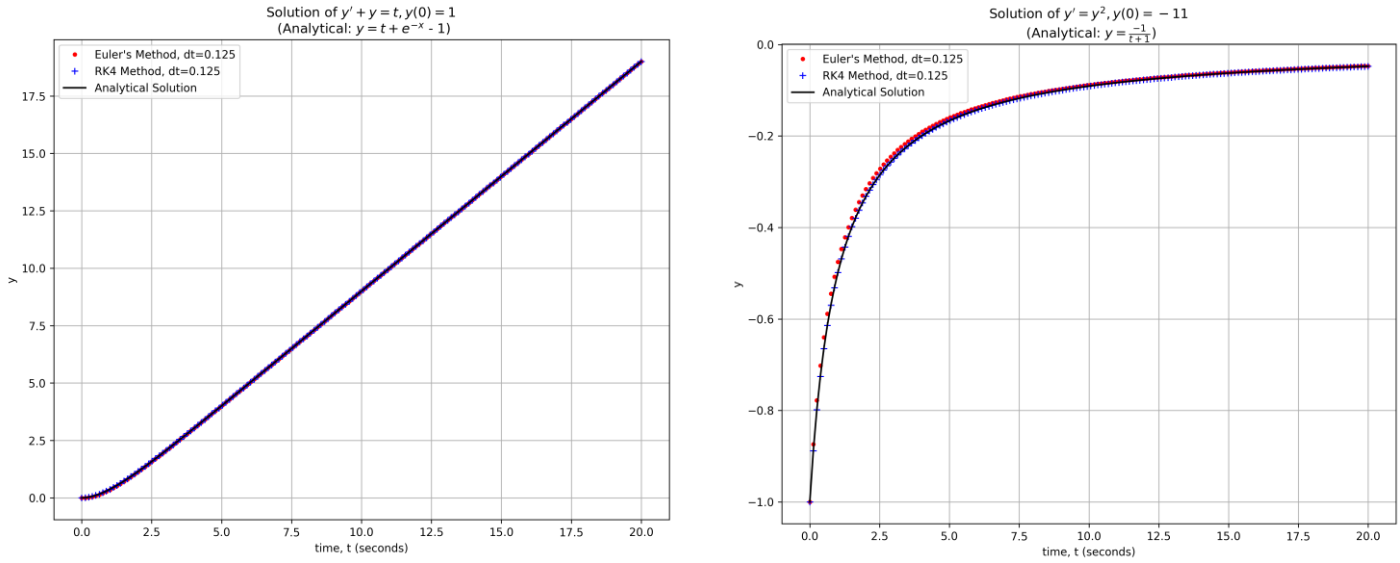

Appendix 1. Comparison – Implementation of the numerical method algorithms vs two known analytical solutions.

APPENDIX 2. Explanation of Files and Code

All files are being submitted in a folder structure, where:

- The source code can be found on the folder 1-source. The source code is supplied in two formats:
    - Python Notebook (ipynb): Recommended for better legibility.
    - Python File (py): Included for compatibility.
- All the generated figures are in the folder 2-figures.
- This report is on the folder 3-report.

Additionally, the files can also be found in an online repository in Github (https://github.com/notidentical/Double-Pendulum-Simulation/).